IDŐJÁRÁS

Quarterly Journal of the Hungarian Meteorological Service
Vol. 115, No. 3, July–September 2011, pp. 147–165

Numerical simulation of the cycle of aerosol particles in stratocumulus clouds with a two-dimensional kinematic model

Beáta Szabó -Takács

University of Pécs, Institute of Environmental Sciences
Ifjúság u. 6, H-7624 Pécs, Hungary;
E-mail: takacs.beata@gamma.ttk.pte.hu

(Manuscript received in final form October 20, 2010)

Abstract—The purpose of the paper was to develop a numerical model to study the cycle of aerosol particles in stratocumulus clouds in different air mass types. A detailed microphysical scheme was incorporated into an idealized two-dimensional kinematic model to investigate the role of the aerosol particles in the formation of the water droplets, regeneration of the aerosol particles due to evaporation of the water drops, and the washout of the aerosol particles. The calculations were made with different cloud condensation nuclei (CCN) size distributions and concentrations typical for maritime, rural, and remote continental air mass types, furthermore, with two different updraft profiles. The water droplets were formed on soluble ammonium-sulfate aerosol particles. The ratio of the number concentration of the soluble and insoluble aerosol particles depended on their size. The drops grew by condensation and collision coalescence in the updraft core, but they evaporated due to the subsaturation in the downdraft region.

The model clearly simulated the regeneration of the aerosol particles. The majority of the water soluble particles were scavenged due to the water drop formation. The efficiency of the scavenging of the water insoluble particles depended on the concentration of the water soluble aerosol particles. While Brownian effect played an important role in capturing these particles, only few of them were washed out due to the phoretic- and gravitational forces. Results of the numerical simulation show that in the case of the stratocumulus clouds the number concentration of insoluble aerosol particles larger than 0.1 μm is hardly modified due to different scavenging mechanisms.

Key-words: aerosol particles, drop formation, condensational growth, collision coalescence, aerosol scavenging, aerosol regeneration

1. Introduction

In the 20th century the interest in the effect of the aerosol particles in the clouds has been increased. The aerosol particles play important role in the formation of the clouds. Their characteristics strongly affect both the optical properties of the clouds and precipitation formation. The impact of aerosol particles on the clouds is strongly affected by the physical and chemical attributes of the particles, which depend on the various air mass types (*Hoose et al.*, 2008; *Sassen et al.*, 1999). While the dynamical processes in general define where supersaturated environments occur in the atmosphere, the cloud attributes are determined by aerosol-cloud interaction (*Targino et al.*, 2007). This interaction includes variety of microphysical processes that affect the concentration, size distribution, and chemical composition of cloud droplets (*Gilliani et al.,* 1995). Clouds play an important role in the redistribution of aerosol particles in the atmosphere. The wet scavenging can be separated into two categories. The in-cloud scavenging refers to nucleation and interstitial scavenging. Another category is the below-cloud scavenging, when the aerosol particles are collected by hydrometeors that fall out from the cloud (*Feng*, 2007). The majority of the water-soluble particles are removed by nucleation scavenging (water drops form on the particle).

Results of numerical simulations about the effect of the size distribution and chemical composition on the albedo and the precipitation formation of the stratocumulus clouds have been published in numerous papers (*Geresdi et al.*, 2006; *Caro et al.*, 2004; *Geresdi* and *Rasmussen*, 2005; *Zhang et al.,* 2004; *Bott*, 2000; *Feingold et al.,* 1996; *Ackerman et al.,* 1995). In our research we have focused on the aerosol–cloud interactions that occur in stratocumulus clouds. Not only the role of the aerosol particles in the precipitation formation was investigated, but also how the water insoluble aerosol particles are washed out. We also studied the regeneration of the aerosol particles in the subsaturated regions.

These processes were investigated in stratocumulus clouds due to their relatively simple dynamics. The weak convective updrafts generate shallow, horizontally extensive cloud layers due to the overlaying drier and stable air that blocks the vertical development of the air mass. Stratocumulus clouds play an important role in climate change due to their high albedo, which causes a significant negative contribution to the overall radiative forcing.

In the present paper we discuss our results on the cycle of the aerosol particles in stratocumulus clouds under different dynamic and environmental conditions.

2. Model description

The microphysical processes that occur in a stratocumulus cloud were simulated in a dynamic framework of the idealized two-dimensional kinematic model developed by *Szumowski et al.* (1998) and *Morrison* and *Grabowski* (2007) with

2D MPDATA routine written by Smolarkiewicz (*Smolarkiewicz* and *Margolin*, 1998). The two-dimensional domain includes both updraft and downdraft regions. The updraft and downdraft regions were characterized with two different maximum velocities. The horizontal and vertical extensions of the domain were 2000 m and 750 m, respectively. The resolution was 20 m in horizontal direction and it was 15 m in vertical direction.

Detailed microphysical scheme was used in the research (see the details in *Geresdi*, 1998; *Geresdi* and *Rasmussen*, 2005). The size distribution of water drops and wet aerosol (haze) particles were divided into 55 bins. At the left side edge of the first bin, the particle mass was 3.048×10^{-20} kg with doubling the mass in the bin edges ($m_{k+1} = 2\, m_k$). The size distribution of the dry aerosol particles were divided into 36 bins. At the left side edge of the first bin, the particle mass was the same in the case of the dry aerosol particles and haze particles (wet aerosol particles). While the density of the aerosol particles was assumed to be size independent (1600 kg/m^3), the density of the haze particles depended on the molar concentration of the solution. The aerosol particles were divided into two categories: water soluble and water insoluble ones. The uncertainties about the size dependence of number concentration of water soluble ammonium-sulfate particles are large. The field observations show that number concentration of the soluble ammonium-sulfate particles comparing with the total aerosol concentration is relatively large in size range of 0.1 μm to 1 μm (*Masahiro et al.*, 2003; *Charlson et al*., 1983; *Kulmala et al.*, 1997; *Mertes et al*., 2005; *Svenningsson et al*., 1997). On the base of these observations the ratio of the number concentration of soluble aerosol particles and the total aerosol particle concentration was chosen to be 0.5 when the radius of the aerosol particles was less than 0.012 μm (in the first 10 bins), and this ratio was 0.7 in case of the larger sizes. The purpose of using external mixture was to investigate the different scavenging mechanisms. The aerosol particles contained water soluble fraction can be washed out mostly by water drop formation (nucleation scavenging). The water insoluble aerosol particles can be collected by water drops through other different scavenging mechanisms (Brownian, phoretic, and gravitational collection).

In this study the following microphysical processes were taken into consideration: (i) drop formation on water soluble aerosol particles, (ii) condensational growth/evaporation of water drops, (iii) collision - coalescence of water drops, and (iv) aerosol particles collection by water drops due to Brownian, phoretics and gravitational motion. Some theoretical studies suggest that the turbulence enhances the water drops – aerosol particles collection efficiency. However, efficient turbulent collection was found for collector drops near 200 μm in combination with particles with diameter of 2–4 μm (*Zhang* and *Vet*, 2006). Because in the stratocumulus clouds the drops size generaly less than 200 μm, the effect of turbulent collision was not taken into account in this study.

The water soluble aerosol particles were transferred into the water drop category, if the relative humidity was larger then 90%. The transfer of dry aerosol particles to wet aerosol particles due to vapor diffusion starts at subsaturated condition. In the case of the small water soluble particles (< 0.1 μm), this process occurred at relative humidity larger than 95%, at larger particles size the transfer occurred at 90%. If the mass of the water in a wet aerosol particle decreased to be equal to the mass of the aerosol inside, the wet aerosol particles were transferred to the dry aerosol particle category. Thirty minutes of cloud life time was simulated using 1 s time step.

The diffusional growth of these particles were calculated by using hybrid bin method. More details about this method can be found in the papers published by *Chen* and *Lamb* (1994) and *Geresdi* and *Rasmussen* (2005). The collision – coalescence processes of water drops were calculated by using two-moments method. These moments – the concentration (N_k) and the mixing ratio (M_k) inside the *k*th bin – were approximated by the following linear equations:

$$N_k(m,t) = f_k \cdot \left(\frac{m_{k+1} - m}{m_{k+1} - m_k} \right) + \psi_k \cdot \left(\frac{m - m_k}{m_{k+1} - m_k} \right) = a_k + b_k \cdot m, \tag{1}$$

$$M_k(m,t) = m_k \cdot f_k \cdot \left(\frac{m_{k+1} - m}{m_{k+1} - m_k} \right) + m_{k+1} \cdot \psi_k \cdot \left(\frac{m - m_k}{m_{k+1} - m_k} \right) = c_k + d_k \cdot m, \tag{2}$$

where m_k and m_{k+1} are the particle mass at the bin boundaries, hereafter m is the mass of the particles. The f and ψ parameters were calculated by using the following equation:

$$M_k^j = \int_{x_k}^{x_{k+1}} m^j n_k(m,t) dx, \tag{3}$$

where M_k^0 and M_k^1 are the concentration (N_k) and mixing ratio (M_k) in the *k*th bin, respectively.

To calculate the kinetic collection equation of water drops, the Smoluchowski equation was used (*Tzivion et al.*, 1999). The water drop – water drop collision efficiencies used in the model are based on the data published by *Hall* (1980). The collision efficiencies for the given sizes of water drops were calculated by linear interpolation. The Brownian motion, the phoretic effect, and the gravitational collection were taken into consideration when the scavenging of the aerosol particles was simulated (*Ackerman et al.*, 1995; *Gwen et al.*, 2004; *Jian*, 2007; *Mircea et al.*, 2000).

The Brownian motion affects the collision between hydrometeors and very small aerosol particles (r_p< 0.01 μm). The following equation gives the number of collected aerosol particles in unit time due to Brownian motion:

$$\left.\frac{dN_p}{dt}\right|_B = 4\pi r_d D_p n_p f_p, \tag{4}$$

where r_d is the radius of the water drop, n_p is the number concentration of the aerosol particles, D_p is the diffusion coefficient for the aerosol particles, f_p is a correction factor which depends on the Reynolds and Schmidt numbers of the aerosol particles (*Pruppacher* and *Klett*, 1997). The motion of aerosol particles due to temperature gradients near to the drop surface is called thermophoresis. Particle motion due to the spatial vapor density gradient is called diffusiophoresis. The sum of the thermophoretic and diffusiophoretic forces is known as phoretic force. The following equation gives the number of collected aerosol particles in unit time due to phoretic forces:

$$\left.\frac{dN}{dt}\right|_{th+df} = \frac{4\pi r_d n_p s f_v}{\left[\frac{L_v}{k_a T_\infty}\left(\frac{L_v}{R_v T_\infty}-1\right)+\frac{R_v T_\infty}{D_v e_s(T_\infty)}\right]}\left(\frac{C}{\rho_a}-\frac{L_v f_{th}}{p}\right), \tag{5}$$

where $s, T_\infty, k_a, p, \rho_a$, and D_v are the supersaturation, temperature, thermal conductivity, pressure, density of air, and diffusivity of vapor in the air, respectively; R_v is the gas constant for the water vapor, L_v is the evaporation heat, e_s is the saturation vapor pressure over flat water surface. f_v and f_{th} represent the ventilation coefficient and thermophoretic force, respectively (*Pruppacher* and *Klett*, 1997). C is the Cunningham-correction, which value depends on the Knudsen number. While in the case of evaporating drop the motion of the aerosol particles is directed toward the surface of the water drop (the right side term in Eq. (5) is larger than zero), in the case of diffusional growth the direction of the motion is opposite (the right side term in Eq. (5) is less than zero). The effect of the phoretic forces is dominant if the size of the aerosol particles is about 0.1 μm (*Wang*, 2002). The phoretic force results in collision between the submicron aerosol particles and the water drops in the subsaturated regions where the drops evaporate. This condition is realized in the precipitation zone and at the lateral edge of the cloud.

If the radius of the aerosol particles is larger than 1 μm, the phoretic forces hardly affect their motion. They are collected by the water drops due to the gravitational collection. The following equation gives the number of aerosol particles collected by a water drop in unit time due to gravitational force:

$$\left.\frac{dN_p}{dt}\right| = E(r_d + r_p)^2 \pi v_t(r_d) n_p, \tag{6}$$

where E is the collection efficiency, r_d and r_p are the radius of the water drop and the aerosol particles, respectively. v_t is the terminal velocity of the water drop.

3. Results

Formation of the water drops and washout of the aerosol particles were examined in the case of three different air mass types: maritime, rural, and remote continental. Initial size distributions of the aerosol particles (*Fig. 1*) were given by equations published by *Jaenicke* (1988). These equations are frequently used in numerical experiments (e.g., *Bott*, 2000; *Leroy et al*., 2006; *Caro et al*., 2004; *Mircea et al*., 2000).

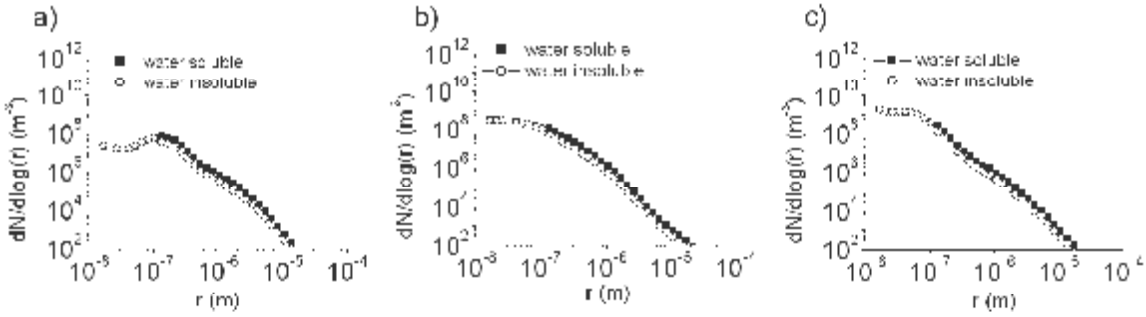

Fig. 1. Initial size distribution of the water soluble (square symbol) and water insoluble (circle symbol) aerosol particles in three different air mass types: (a) maritime, (b) rural, and (c) remote continental.

The spatial distribution of the supersaturation gives information about the development of the cloud. In addition, the phoretic force depends on the subsaturation (see Eq. (5)). The supersaturation is affected by the adiabatic rising of the moist air and by the formation and condensational growth of water drops (*Cohard et al*., 1998). The supersaturation rapidly increases above the cloud base until it reaches its maximum value. Thereafter it decreases gradually, and at about 100 m above the cloud base it becomes near constant. Most of the haze particles reach their critical size in the updraft region, near to the cloud base where supersaturation is the largest. *Fig. 2* shows the simulated vertical profile of the supersaturation at 0.5 m/s and 1.2 m/s maximum updraft velocities at different aerosol concentrations.

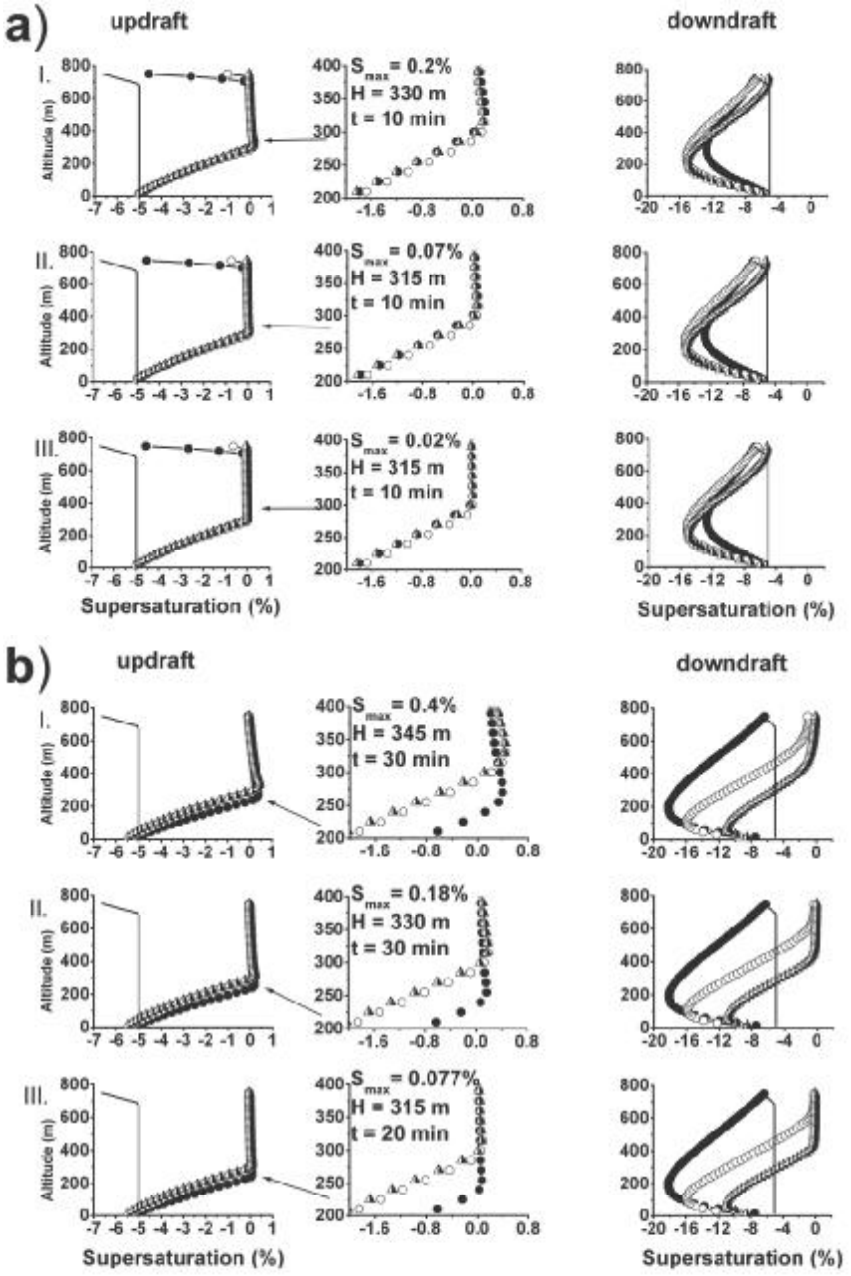

Fig. 2. Vertical profile of the supersaturation in case of maritime (I), rural (II), and remote continental (III) air masses at t = 10 min (black cycle), t = 20 min (white cycle) and t = 30 min (black and white triangle) according to initial supersaturation (solide line) at maximum updraft velocity of 0.5 m/s (a) and 1.2 m/s (b).

In case of weaker maximum updraft velocity (w_{max} = 0.5 m/s), the supersaturation reached its maximum value at about 300 m above the surface, and after a small diminution it became nearly constant with increasing altitude. The largest maximum supersaturation value occurred in the case of the maritime air mass, because the low CN concentration resulted in lower concentration of droplets. Above the cloud top, the saturation suddenly decreased in all

simulation times. With increasing time, reduction rate decreased. In the downdraft region, the relative humidity decreased at lower altitude. After 30 minute of simulation time, the rate of the depletion significantly decreased. Below the cloud base, the relative humidity slightly increased due to the evaporation of falling droplets.

When the maximum updraft velocity was stronger ($w_{max} = 1.2$ m/s) the maximum supersaturation occurred at lower altitude at the beginning (10th minute) than in the case of weaker maximum updraft. With increasing time, the position of the maximum of the supersaturation rose to higher altitude. In the downdraft core, the relative humidity depended on the adiabatic descend of the air and the evaporation of the water drops. While the warming due to adiabatic descend reduces the relative humidity, the evaporation of the water drops increases it. The decrease of the relative humidity until about the 10th minute of the simulation was the consequence of the dry adiabatic descend of the air. The appearance of water drops after the 10th minute resulted in increase of the relative humidity everywhere in the downdraft. This explains that the relative humidity was lower in the case of stronger updraft until the 10th minute of the simulation than in the case of weaker updraft. The increase of the relative humidity was the consequence of the evaporation of the water drops in the down draft core. While this process confined to near to the top of the domain in the case of weaker updraft, evaporation of the water drops occurred in an about 400 m deep layer in the case of the stronger updraft. (See the layer where the supersaturation is eaqual to zero in the right coloumn in *Fig. 2b.*) The effect of evaporation was the largest in the case of remote continental air mass type (IIIrd row in *Fig. 2b.*). This can be explained by the fact, that the total surface area of the water drops was the largest in this case.

Some features of simulation are summarized in *Tables 1* and *2*. The domain integrated number concentration or mixing ratios (*M*), furthermore, the domain and time integrated production terms (*P*) were calculated by the following equation:

$$M = \sum_{i,j} M_{i,j} \rho_a \Delta x \Delta y, \qquad P = \sum_{n=1}^{n_{\max}} \Delta t \sum_{i,j} p_{i,j}\, \rho_a \Delta x \Delta y, \tag{7}$$

where Δx and Δy are the horizontal and vertical distances between the grid points, respectively, ρ_a is the density of air, Δt is the time step, $n_{\max}$ is the number of time steps used during the simulation; $p_{i,j}$ is the production term calculated at the grid point i, j and $M_{i,j}$ is the number concentration or the mixing ratio of the aerosol particles.

Table 1 shows the time and domain integrated production term for the condensation of vapor, change of the number concentration, mixing ratio and

aerosol mass of the wet aerosol particles due to condensation, and the change of the concentration of the water drops due to the collision-coalescence.

Table 1. The following domain integrated production term: change of the mass of wet aerosol particles-water drops due to condensation (ΔM_c); transfer of the dry aerosol particles to wet aerosol particles due to the increase of the relative humidity. Number (column a), mass of water plus aerosol (column b), only aerosol mass (column c); decrease of the number of the water drops due to drop-drop collision

	ΔM_c	N **(a)**	M_w **(b)**	M_a **(c)**	N_w	**Updraft**
	(kg m^{-1})	(m^{-1})	(kg m^{-1})	(kg m^{-1})	(m^{-1})	m/s
Maritime	1.31×10^2	9.54×10^{13}	4.80×10^{-2}	2.40×10^{-2}	-4.50×10^{11}	
Rural	1.31×10^2	4.43×10^{14}	5.37×10^{-2}	2.68×10^{-2}	-4.45×10^{11}	0.5
Remote continental	1.31×10^2	2.02×10^{15}	6.19×10^{-2}	3.09×10^{-2}	-3.81×10^{11}	
Maritime	2.07×10^2	9.72×10^{13}	4.80×10^{-2}	2.40×10^{-2}	-1.84×10^{12}	
Rural	2.09×10^2	4.62×10^{14}	5.37×10^{-2}	2.68×10^{-2}	-1.42×10^{12}	1.2
Remote continental	2.11×10^2	2.12×10^{15}	6.21×10^{-2}	3.10×10^{-2}	-1.08×10^{12}	

The increase of the total water content was caused by the condensational growth of the wet aerosol particles and water drops. Both the wet aerosol particles and water drops evaporated in the subsaturated region. Similarly to the results published by *Szumowski* et al. (1998), our results show that the water drops, that remained in the updraft core, permanently grow, and the water drops that fall out from the updraft into the outflow, remain small, or completely evaporate. This is demonstrated by the joint size distributions of the water drops and of wet aerosol particles in *Figs. 3* and *4*. The mean size of the water drops increases in the updraft core and decreases in the downdraft regions. Another important feature of the size distributions is that while they were getting narrower in the ascending air due to the condensational growth of the water drops and due to the evaporation of the wet aerosol particles which did not reach the critical size, they got wider due to the evaporation of the water drops in the downdraft. Near to the surface in the downdraft region, the size distribution should be similar to that of the initial size distribution of the aerosol particles due to the complete evaporation of the water drops. The differences can be the consequence of the following reasons: (i) some of the water soluble aerosol particles can be captured by the water drops due to different scavenging mechanisms; (ii) numerical deficiency. During the calculation, the discrete bin width limits the information about the mass of the aerosol particle inside of the drops. This uncertainty of the mass of aerosol particles inside the water drops caused fluctuations in the number concentration of the regenerated aerosol particles at the submicron size in the downdraft core. To avoid this effect, the size distribution can be smoothed by calculation of the mean value of the concentration in three neighboring bins (n_{k-1}, n_k, n_{k+1}) (*Geresdi* and *Rasmussen*, 2005).

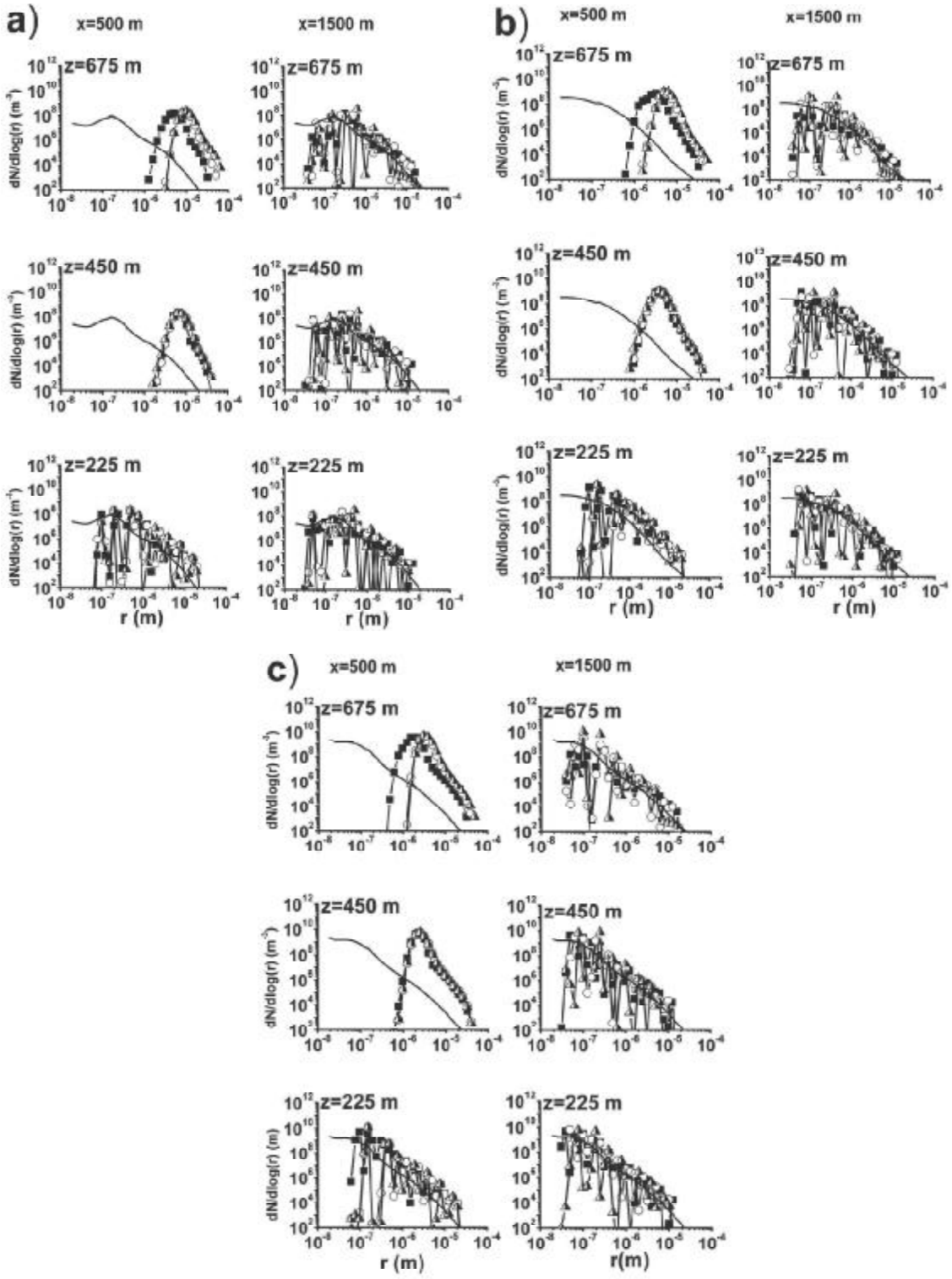

Fig. 3. The evolution of size distribution of the water drops in maritime (a), rural (b) and remote continental (c) air masses at t = 10 min (black square), at t = 20 min (white cycle) and at t = 30 min (black and white triangle) according to initial size distribution of water soluble aerosol particles at 0.5 m/s maximum updraft velocity in the updraft core (x = 500 m) and in the downdraft core (x = 1500 m).

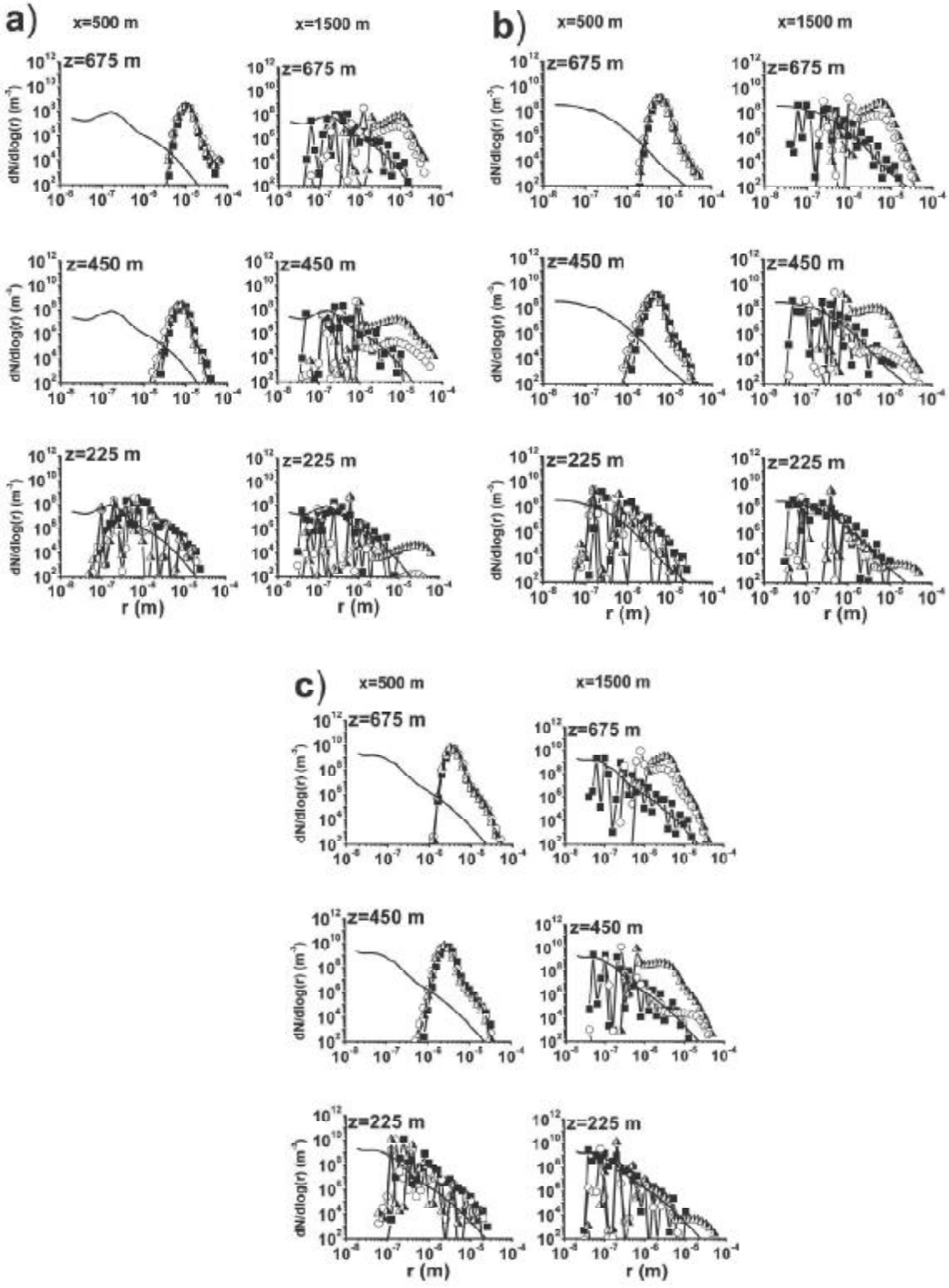

Fig. 4. The evolution of size distribution of the water drops in maritime (a), rural (b) and remote continental (c) air masses at t = 10 min (black square), t = 20 min (white cycle) and t = 30 min (black and white triangle) according to initial size distribution of water soluble aerosol particle at maximum updraft velocity of 1.2 m/s in the updraft core (x = 500 m) and in the downdraft core (x = 1500 m).

The initial size distribution of the water soluble aerosol particles significantly affects the size distribution of the water drops form on them. The concentration of the water drops less than 25 μm was the smallest in the case of maritime air mass and it was the largest in the case of remote continental one (*Fig. 5*).

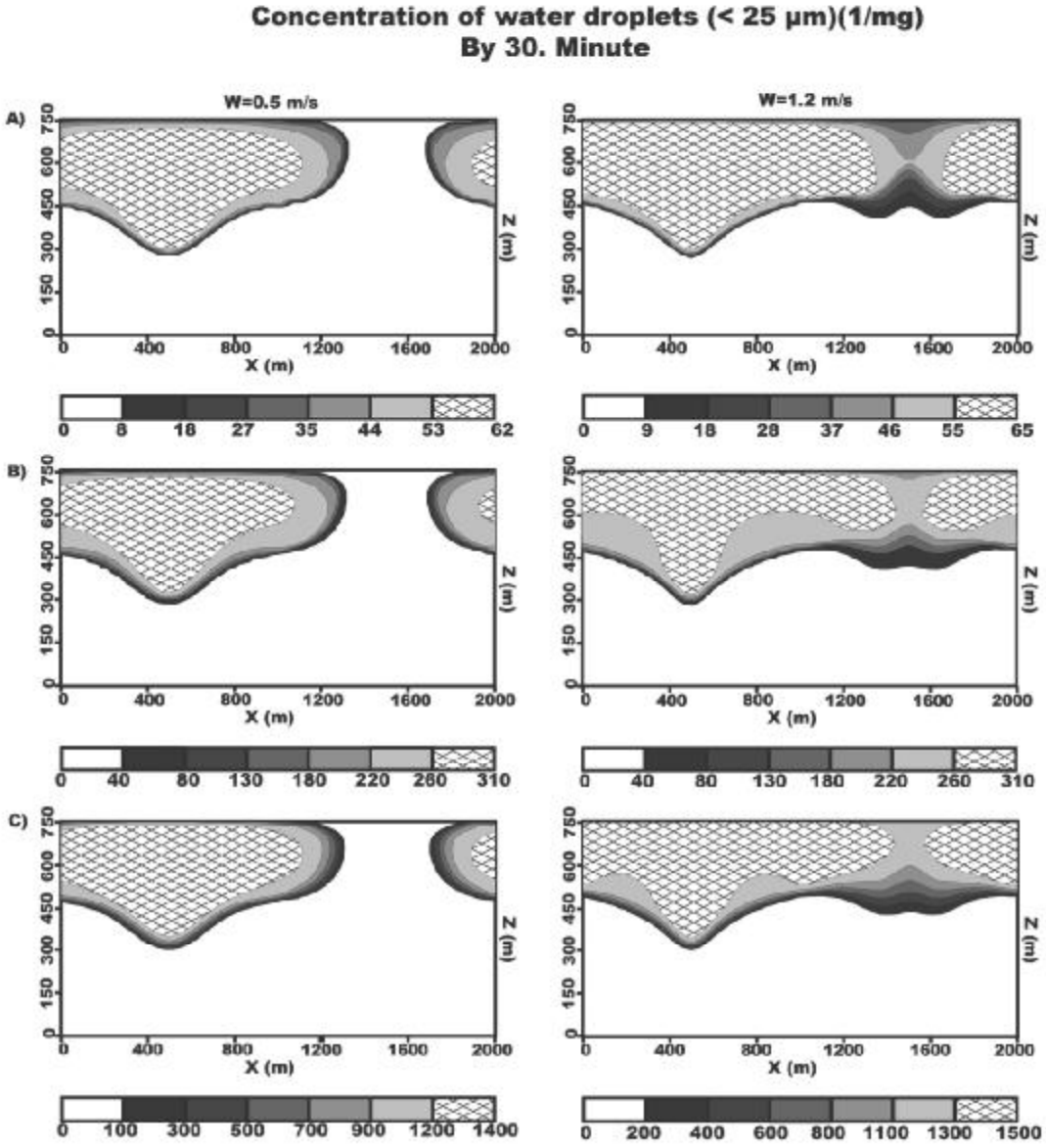

Fig. 5. The evolution of size distribution of the water drops in maritime (a), rural (b), and remote continental (c) air masses at maximum updraft velocity of 0.5 and 1.2 m/s.

Due to the small concentration of water soluble aerosol particles less water drops formed in the maritime airmass. Hence, more water vapor condensed on each of these drops. As a result, the mean mass of drops was larger in the maritime airmass than in the rural and remote continental airmasses. This result was reported also by *Leroy et al*. (2006), *Reisin et al*. (1996), and *Rasmussen et*

al. (2002). As the efficiency of the collision-coalescence of the water drops strongly depends on the mean size of the drops, the concentration of the drizzle size water drops ($r > 25$ μm) was the highest in the maritime case. The mixing ratio of these drops was ten times larger in the maritime case than in the rural air mass case (*Fig. 6*). The water drops were rising until their terminal velocity was equal to the vertical velocity of air and, thereafter, they began to fall down. The fall-out of the rain drops began earlier in the maritime air mass due to the larger terminal velocity of the rain drops.

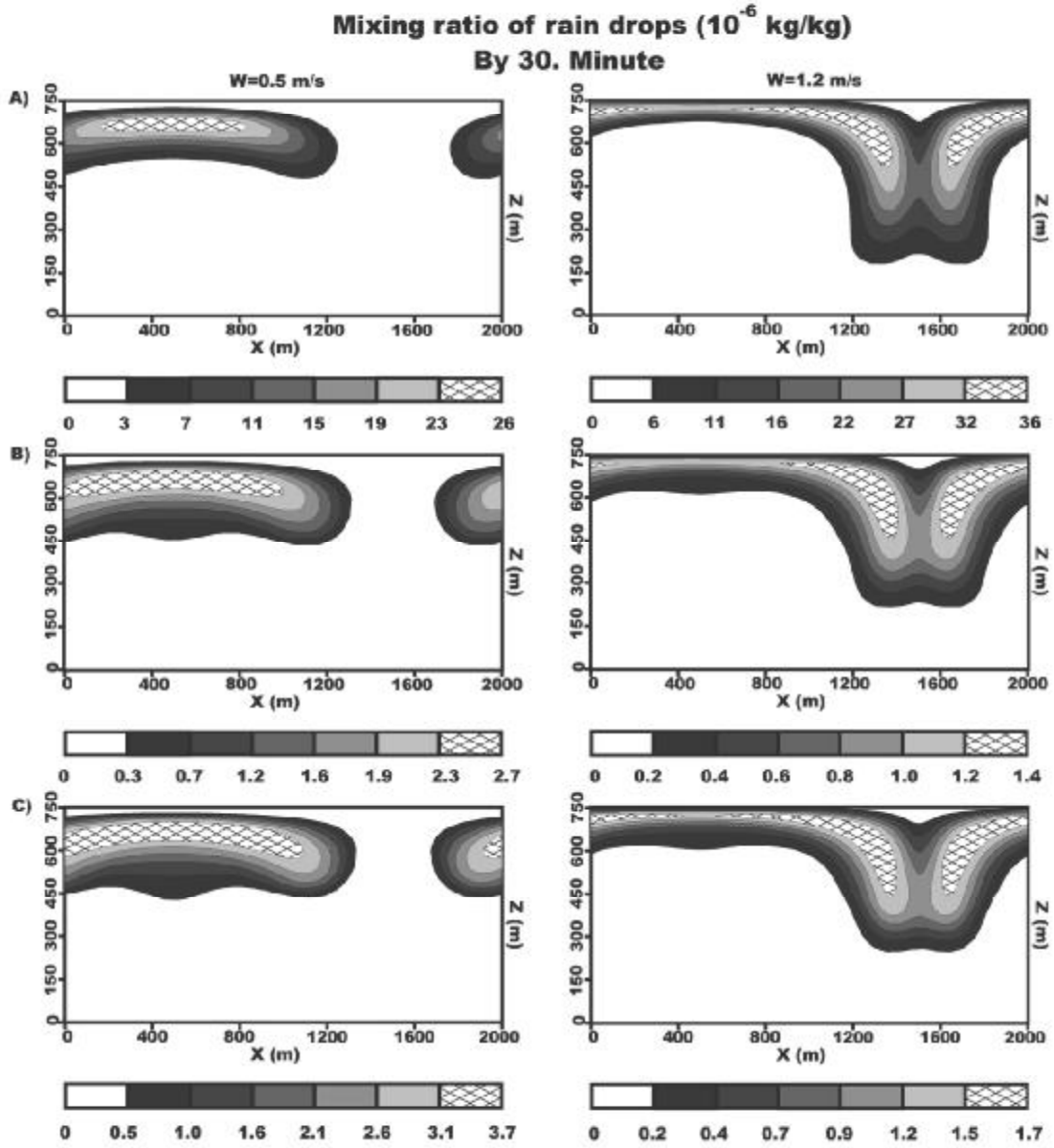

Fig. 6. Mixing ratio of the rain drops in maritime (a), rural (b), and remote continental (c) air mass types at two different maximum updraft velocities by the end of simulation. Scale is given in kg/kg.

Table 2 shows the domain and time integrated values of the production terms, that give the change of number and mass of the water soluble and water insoluble aerosol particles due to Brownian and phoretics effects.

Table 2. Domain and time integrated value of the change of concentration (ΔN_s) and mixing ratio (ΔM_s) of water soluble and insoluble (ΔN_{is}, ΔM_{is}) aerosol particles due to Brownian and phoretic collision with water drops, initial domain integrated concentration and mixing ratio of the water soluble and insoluble aerosol particles

	ΔN_s (m^{-1})	ΔM_s (kg m^{-1})	ΔN_{is} (m^{-1})	ΔM_{is} (kg m^{-1})	**Updraft** m/s
Maritime	-6.09×10^{8}	-3.65×10^{-10}	-6.33×10^{11}	-5.55×10^{-6}	
Rural	-1.22×10^{10}	-3.26×10^{-9}	-1.36×10^{13}	-1.40×10^{-5}	0.5
Remote continental	-5.59×10^{10}	-1.45×10^{-8}	-1.45×10^{14}	-6.69×10^{-5}	
Maritime	-4.98×10^{8}	-2.97×10^{-10}	-1.35×10^{12}	-7.87×10^{-6}	
Rural	-9.69×10^{9}	-2.56×10^{-9}	-3.03×10^{13}	-3.27×10^{-5}	1.2
Remote continental	-4.48×10^{10}	-1.16×10^{-8}	-3.03×10^{14}	-1.43×10^{-4}	
	N_{s0} (m^{-1})	M_{s0} (kg m^{-1})	N_{is0} (m^{-1})	M_{is0} (kg m^{-1})	
Maritime	9.86×10^{13}	2.40×10^{-2}	6.60×10^{13}	8.34×10^{-3}	
Rural	4.75×10^{14}	2.69×10^{-2}	4.28×10^{14}	9.52×10^{-3}	0.5
Remote continental	2.19×10^{15}	3.11×10^{-2}	2.11×10^{15}	1.19×10^{-2}	
Maritime	9.86×10^{13}	2.40×10^{-2}	6.60×10^{13}	8.34×10^{-3}	
Rural	4.75×10^{14}	2.69×10^{-2}	4.28×10^{14}	9.52×10^{-3}	1.2
Remote continental	2.19×10^{15}	3.11×10^{-2}	2.11×10^{15}	1.19×10^{-2}	

For the depletion rate of aerosol particle due to nucleation scavenging we got similar result to that of published by *Zhang et al.* (2004). They investigated aerosol scavenging by low-level, warm stratiform clouds and precipitation using a one-dimensional model with detailed cloud microphysics and size resolved aerosol particles and hydrometeors. By the end of the simulation, more than 90% of the water soluble aerosol particles and more than 99% of the mass of the water soluble aerosol particles were depleted due to the formation of water drops in each case. The rate of condensation increased with the strength of the updraft. Negligible fraction of water soluble particles was scavenged due to the Brownian and phoretics effects. These results also agree with that of published by *Zhang et al.* (2004). *Fig. 7* shows the time integrated change of the concentration of the water insoluble aerosol particles in the case of 0.5 m/s and 1.2 m/s maximum updraft velocities by the 30th minute of the simulation. In case of smaller clouds (weaker updraft) the aerosol particles were scavenged just inside the clouds. While in case of larger clouds (stronger updraft) the drops collected the particles at the edge of clouds and in the downdraft core too. Collection was most significant in the upper divergence region. The high collection rate in the remote continental and rural airmass was the consequence of the larger total surface area of the droplets in a unit volume of the air.

Comparing the initial and final size distributions of the aerosol particles, the total number of water insoluble aerosol particles decreased by 1% and 2% in the case of maritime airmass, 3% and 7% in the case of rural airmass, and 7% and 14% in the case of remote continental airmass at maximum vertical velocities of 0.5 m/s and 1.2 m/s, respectively.

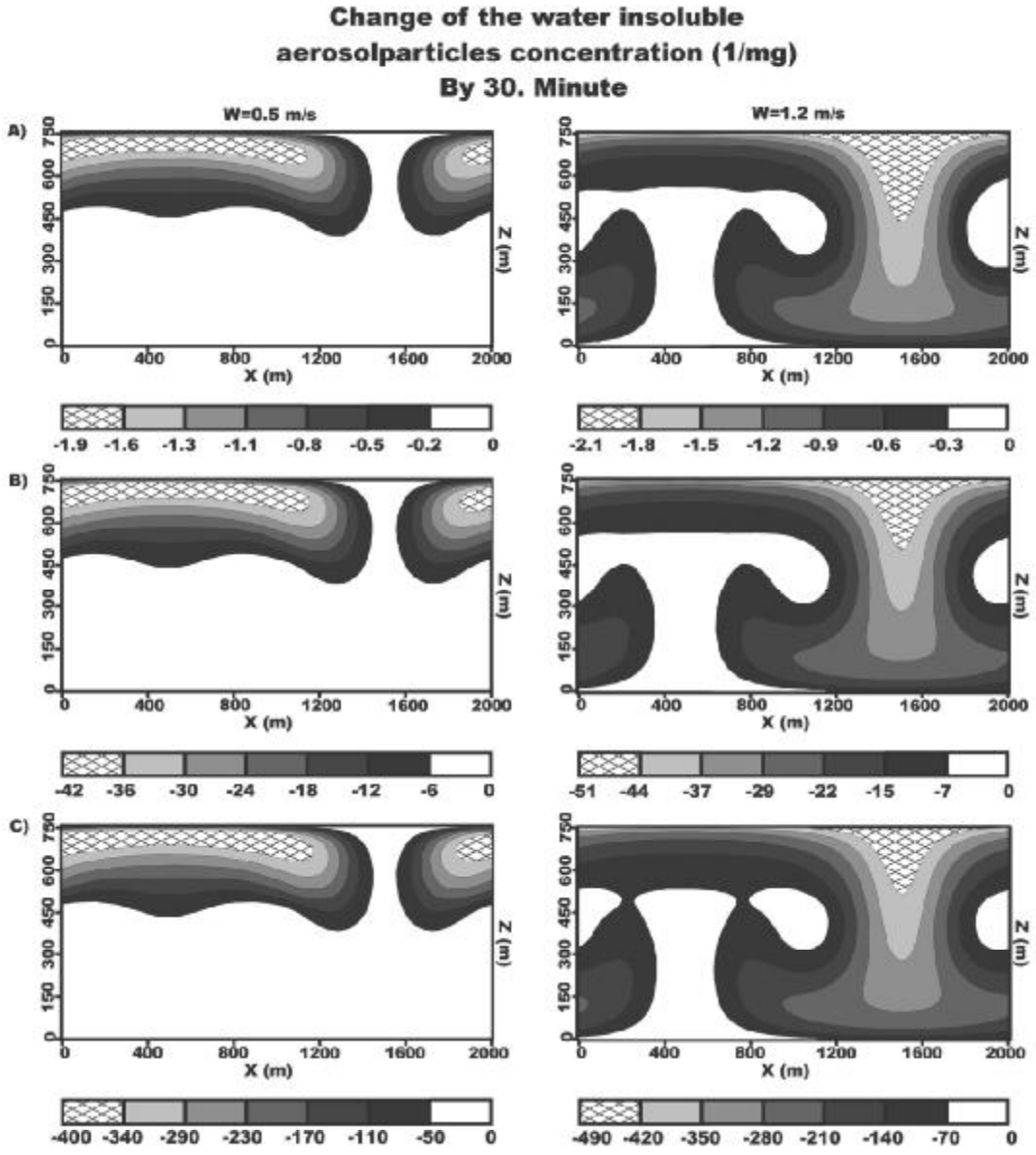

Fig. 7. Concentration of the water droplets in maritime (a), rural (b), and remote continental (c) air mass types at two different maximum updrafts velocities by the end of the simulation. Scale is given in 1/mg.

The reduction in mass of the water insoluble aerosol particles was just a few tenth percents in each case. It follows from the fact that relatively more small particles were collected than large ones. The relative efficiency of scavenging of

the aerosol particles less than 0.1 μm means that scavenging of the water insoluble particles was mostly governed by the Brownian effect inside the cloud.

To investigate the efficiency of the scavenging in different regions of the domain, the following equation was calculated:

$$Scav_{eff} = \frac{N_0 - N_t}{N_0}, \tag{8}$$

where N_0 and N_t are the number concentration of the aerosol particles at a given grid point at the beginning and the end of the simulation, respectively. *Figs. 8a* and *8b* show the efficiency of scavenging in the case of remote continental airmass, when the maximum of the updraft velocity was 0.5 m/s and 1.2 m/s, respectively.

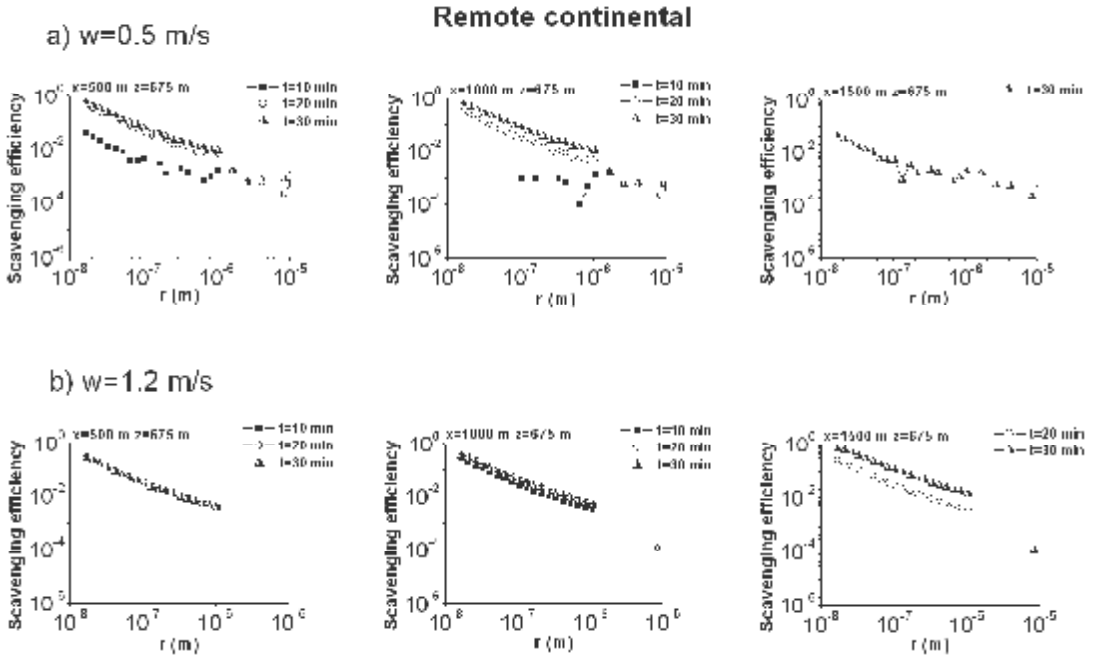

Fig. 8. Collection efficiency of the Brownian, phoretic, gravitational and dynamical processes at maximum updraft velocities of 0.5 m/s (a) and 1.2 m/s (b) in the remote continental airmass at three different grid points.

The three grid points represent three different regions of the domain. The left side figures in *Figs. 8a* and *8b* represent the updraft region near to the top of the cloud. Figures at x = 1000 m represent the cloud region where only horizontal flow occurs. The right side figures show the scavenging efficiency in the downdraft regions. It is clearly shown that the steepness of the curves is very similar at different grid points and at different maximum updraft velocities, as well. The difference between *Figs. 8a* and *8b* indicates that it takes longer time to reach the steady state in the case of weaker updraft. The aerosol particles less

than 0.1 μm were collected most efficiently by Brownian motion. The effect of Brownian motion strongly decreased above this particle size (*Young*, 1974). In the size range of 0.1 μm to 1 μm, only less than 1 percent of the particles were scavenged due to phoretic forces. The effect of the gravitational force was negligible. This force would have changed the concentration of the micron size particles considerably if the size of the hydrometeor had reached the value of 100–200 μm.

4. Summary

The aim of our research was to study the cycle of aerosol particles in stratocumulus clouds using a detailed microphysical scheme in the case of maritime, rural, and remote continental air mass types and at different dynamic conditions. In this study we focused on the following processes:

4.1. Drop formation and regeneration of aerosol particles

The model was able to simulate the regeneration of the water soluble aerosol particles. Neglecting the effect of numerical deficiency caused by the limits of information about the mass of the aerosol particle inside of the drops, the initial size distribution of the water soluble aerosol particles and the size distribution of the regenerated aerosol agree well.

The size distribution of the wet aerosol particles was mostly affected by the nucleation scavenging. Because the mean drop size was relatively small even in the case of maritime airmass, the collision-coalescence of the water drops hardly affected the size distribution of the regenerated aerosol particles.

4.2. Scavenging of water soluble and water insoluble aerosol particles

The water soluble aerosol particles diminished more than 90% in number and more than 99% in mass during the drop formation. Only about 0.1% of the water soluble particles were collected due to Brownian and phoretic forces.

The efficiency of scavenging of water insoluble aerosol particles depended on the initial concentration of the water soluble aerosol particles and on the intensity of the updraft.

Depending on the initial concentration of aerosol particles and the intensity of the updraft, about from 1 to 14% of the insoluble aerosol particles were collected by the different scavenging processes. In the case of more intense updraft, the aerosol particles were removed most efficiently in the downdraft core. The decrease of the number concentration was most significant in the size range of 0.01–0.1 μm due to the Brownian motion.

The results of numerical simulation show that phoretic effects hardly affect the washout of the aerosol particles in the case of the precipitable stratocumulus.

Thus the aerosol particles which do not contain water soluble fraction and their size is between 0.1 and 1.0 μm can have a relative long atmospheric retention time. Further research about how the other cloud types with more efficient precipitation formation can affect the washout these particles is necessary.

***Acknowledgements*—**I would like to thank to *Dr. István Geresdi* for his contribution to the present work and for reviewing the manuscript, and also for using his numerical code. I also should like to thank to the anonymous reviewers for their comments and suggestions.

References

Ackerman, A.S., Toon, O.B., Hobbs, P.V., 1995: A model for particle microphysics, turbulent mixing, and radiative transfer in the stratocumulus-topped marine boundary layer and comparisons with measurements. *J. Atmos. Sci. 52*, 1204-1236.

Bott, A., 2000: A numerical model of cloud-topped planetary boundary-layer: influence of the physico-chemical properties of aerosol particles on effective radius of statiform clouds. *Atmos. Res. 53*, 15-27.

Caro, D., Wobrock, W., Flossmann, A.I., Chaumerliac, N., 2004: A two-moment parametrization of aerosol nucleation and impaction scavenging for a warm cloud microphysics: description and results from two-dimensional simulation. *Atmos. Res. 70*, 171-208.

Charlson, R.J., Vong, R., Hegg, D.A., 1983: The sources of sulphate in precipitation: 2. Sensitivities to chemical variables. *J. Geophys. Res. 88*, 1375-1377.

Chen, J.P., Lamb, D., 1994: Simulation of cloud microphysical and chemical processes using multicomponent framework. Part I: Description of the microphysical model. *J. Atmos. Sci. 51*, 2613-2630.

Cohard, J.M., Pinty, J., Bedos, C., 1998: Extending Twomey's analytical estimate of nucleated cloud droplet concentration from CCN spectra. *J. Atmos. Sci. 55*, 3348-3357.

Feingold, G., Heymsfield, A.J., 1992: Parametrizations of condensational growth of droplets for use in general circulation models. *J. Atmos. Sci. 49*, 2325-2342.

Feingold, G., Kreidenweis, S.M., Stevens, B., Cotton, W.R., 1996: Numerical simulations of stratocumulus processing of cloud condensation nuclei through collision-coalescence. *J. Geophys. Res. 101*, 21.391-21.402.

Feng, J., 2007: A 3-mode parametrization of below-cloud scavenging of aerosols for use in atmospheric dispersion models. *Atmos. Environ. 41*, 6808-6822.

Geresdi, I., 1998: Idealized simulation of the Colorado hailstorm case: comparison of bulk and detailed microphysics. *Atmos. Res. 45*, 237-252.

Geresdi, I., Rasmussen, R., 2005: Freezing drizzle formation in stably stratified layer clouds. Part II: The role of giant nuclei and aerosol particle size distribution and solubility. *J. Atmos. Sci. 62*, 2037-2057.

Geresdi, I., Mészáros, E., Molnár, A., 2006: The effect of chemical composition and size distribution of aerosol particles on droplet formation and albedo of stratocumulus clouds. *Atmos. Environ. 40*, 1845-1855.

Gilliani, N.V., Schwartz, S.E., Leaitch, W.R., Strapp, J.W., Isaac, G.A., 1995: Field observations in continental stratiform clouds: Partitioning of cloud particles between droplets and unactivated interstitial aerosols. *J. Geophys. Res. 100*, 18.687-18.706.

Gwen, A., Cederwall, R.T., 2004: Precipitation scavenging of atmospheric aerosols for emergency response applications: testing an updated model with new real-time data. *Atmos. Environ. 38*, 993-1003.

Hall, W.D., 1980: A detailed microphysical model within a two-dimensional dynamic framework: model description and preliminary results. *J. Atmos. Sci. 37*, 2486-2507.

Hoose, C., Lohmann, U., Bennartz, R., Croft, B., Lesins, G., 2008: Global simulation of aerosol processing in clouds. *Atmos. Chem. Phys. Discuss. 8*, 13.555-13.618.

Jaenicke, R., 1988: Aerosol physics and chemistry. In *Zahlenwerte und Funktionen aus Naturwissenschaften und Technik*. (ed.: *L. Boernstein) 4b*, 391-457, Springer-Verlag.

Kulmala, M., Korhonen, P., Laaksonen, A., Charlson, R.J., 1997: A generalized reformulation of Köhler theory: Effects of soluble trace gases and slightly soluble substances. *J. Aeros. Sci. 28*, S749-S750.

Leroy, D., Monier, M., Wobrock, W., Flossmann, I.A., 2006: A numerical study of the effect of the aerosol spectrum on the development of the ice phase and precipitation formation. *Atmos. Res. 80*, 15-45.

Masahiro, H., Sachio, O., Naoto, M., Sadamu, Y., 2003: Activation capability of water soluble organic substances as CCN. *J. Aeros. Sci. 34*, 419-448.

Metres, S., Galgon, D., Schwirn, K., Nowak, A., Lehmann, K., Massling, A., Wiedensohler, A., Wieprecht, W., 2005: Evolution of particle concentration and size distribution observed upwind, inside and downwind hill cap clouds at connected flow conditions during FEBUKO. *Atmos. Environ. 39*, 4233-4245.

Mircea, M., Stefan, S., Fuzzi, S., 2000: Precipitation scavenging coefficient: influence of measured and raindrop size distributions. *Atmos. Environ. 34*, 5169-5174.

Morrison, H., Grabowski, W.W., 2007: Comparison of bulk and bin warm-rain microphysics models using kinematic framework. *J. Atmos. Sci. 64*, 2839-2861.

Pruppacher, H.R., Klett, J.D., 1997: *Microphysics of Clouds and Precipitation*. Kluwer Academic Publishers, Dordrecht/Boston/London.

Rasmussen, R., Geresdi, I., Thompson, G., Manning, K., Karplus, E., 2002: Freezing drizzle formation in stably stratified layer clouds: The role of radiative cooling of cloud droplets, cloud condensation nuclei and ice initiation. *J. Atmos. Sci. 59*, 837-860.

Reisin, T., Levin, Z., Tzivion, S., 1996: Rain production in convective clouds as simulated in an axisymmetric model with detailed microphysics. Part II: Effect of varying drops and ice initiation. *J. Atmos. Sci. 53*, 1815-1837.

Sassen, K., Mace, G.G., Wang, Z., Poellot, M.R., Sekelsky, S.M., McIntosh, R.E., 1999: Continental stratus clouds: A case study using coordinated remote sensing and aircraft measurements. *J. Atmos. Sci. 56*, 2345-2358.

Smolarkiewicz, K.P. and *Margolin, L.G.*, 1998: MPDATA: A finite-difference solver for geophysical flows. *J. Comput. Phys. 140*, 459-480.

Svenningsson, B., Hansson, H., Martinsson, B., Wiedensohler, A., Swietlicki, E., Cederfelt, S., Wendish, M., 1997: Cloud droplet nucleation scavenging in relation to the size and hygroscopic behavior of aerosol particles. *Atmos. Environ. 31*, 2463-2475.

Szumowski, M.J., Grabowski, W.W., Ochs, H.T., 1998: Simple two-dimensional kinematic framework designed to test warm rain microphysical models. *Atmos. Res. 45*, 299-326.

Targino, A.C., Noone, K.J., Drewnick, F., Schneider, J., Krejci, R., Olivares, G., Hings, S., Borrmann, S., 2007: Microphysical and chemical characteristics of cloud droplet residuals and interstitial particles in continental stratocumulus clouds. *Atmos. Res. 86*, 225-240.

Tzivion, S. Reisin, T.G., Levin, Z., 1999: A numerical solution of kinetic collection equation using high spectral grid resolution: a proposed reference. *J. Comput. Phys. 148*, 527-544.

Wang, P.K., 2002: Sharpe microdynamics of ice particle and their effect, in cirrus clouds. In: *Advances in Geophysics* (eds.: *R. Dmowska, B. Saltzman*) *45.* Academic Press.

Young, K.C., 1974: The role of contact nucleation in ice phase initiation in clouds. *J. Atmos. Sci. 31*, 768-776.

Zhang, L., Michelangeli, D.V., Taylor, P.A., 2004: Numerical studies of aerosol scavenging by low-level, warm stratiform clouds and precipitation. *Atmos. Environ. 38*, 4653-4665.

Zhang, L., Vet, R., 2006: A review of current knowledge concerning size- dependent aerosol removal. *China Particuol 4*, 272-282.